



Synthesis and structure of five or six-coordinate manganese deuteroporphyrin-niacin dyads with intramolecular axial pyridine

Chengguo Sun, Bingcheng Hu*, Donghui Zhao, Zuliang Liu

School of Chemical Engineering, Nanjing University of Science and Technology, Nanjing, Jiangsu Province 210094, China

ARTICLE INFO

Article history:

Received 15 June 2012

Received in revised form

9 July 2012

Accepted 13 July 2012

Available online 20 July 2012

Keywords:

Porphyrin-niacin dyads

Deuteroporphyrin

Niacin

Axial coordination

Manganese porphyrin

Intramolecular action

ABSTRACT

Deuteroporphyrin-niacin dyads with different chain lengths have been synthesized by modification of the propionate side chains of hemin. When a manganese ion was inserted into the porphyrin core, the UV spectral shift of manganese deuteroporphyrin-niacin dyads were experimentally demonstrated to mainly originate from the intramolecular coordination. In order to elaborate the intramolecular coordination, the spectra of single manganese porphyrin complexes in CH_2Cl_2 solution were measured and compared to that of the addition of axial ligands (pyridine and methyl nicotinate). Among all the synthetic dyads, the compounds of 2,7,12,18-tetramethyl-13,17-di(3-hydroxypropyl nicotinate) porphyrin and 2,7,12,18-tetramethyl-13,17-di(3-aminoethyl nicotinate) porphyrin manganese bearing the short chains did not show intramolecular coordination of the terminal base on the metal ion. Other three compounds of the niacin moiety indirectly bonded to the propionate side chains of manganese porphyrin through the diols linkage exhibited optical spectra characteristic of five or six-coordinate manganese complexes. These results indicate that the niacin groups' access to the Mn(III) center depended on the chain lengths.

Crown Copyright © 2012 Published by Elsevier Ltd. All rights reserved.

1. Introduction

Heme, a unique porphyrin compound and niacin have been extensively studied as typical N-heterocyclic compounds [1–4]. The former is considered as the prosthetic group of cytochrome P450 enzymes and is used in a wide range of fields including photodynamic therapy, supramolecular self-assembly, and biomimetic catalytic oxidation [5,6]. The latter is a component of vitamin B₃, which is one of the oldest drugs used to treat dyslipidemia [7,8]. Both of the compounds have distinctive structures and predominant physical, chemical, and optical properties, and are valuable in potential applications in biological science, biochemistry and medical chemistry.

During the last decades, many researchers have put great efforts into the synthesis of porphyrin and niacin compounds, especially for the multiple porphyrin or niacin complexes linked with bioactive substances [9–11]. Therefore, synthesis of the porphyrin covalently bonded with niacin is worthy of further investigation. Additionally, the porphyrin-niacin dyads can be used as a building block of supermolecular assembly by coordination bonding interactions through N atoms of niacin with other materials [12,13]. They

can also serve as the intramolecular or intermolecular coordination between the niacin and central metal ion [14–16], which is one way to achieve novel biomimetic catalysts with high activity and stability.

As part of our continuing goal to develop new methods for the preparation of biologically active heterocyclic compounds, we have recently focused on improving the synthesis of porphyrin by modification of natural hemin, as the extract of natural heme. In order to study the distance dependence of intramolecular coordination between the central metal ion of metalloporphyrin and the niacin, we synthesized a series of porphyrin-niacin dyads by modification of the propionate side chains of hemin (Schemes 1–3). Two niacin molecules are covalently bonded through two flexible chains of varying lengths to the tail of deuteroporphyrin (DP) in these molecules.

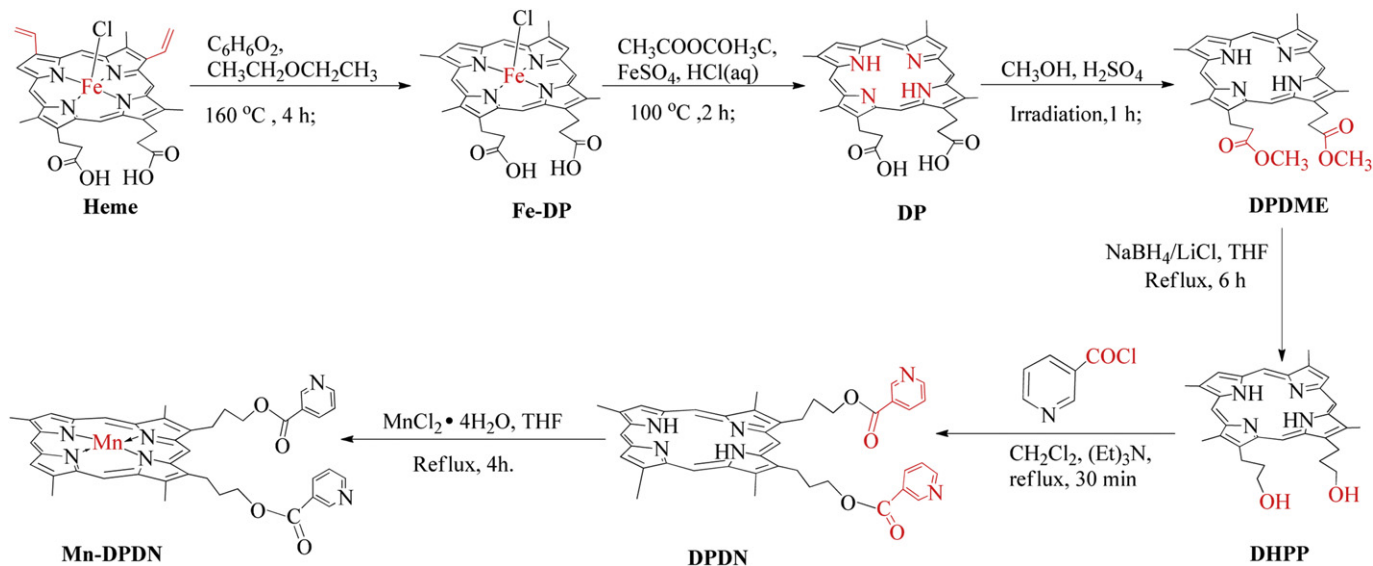
2. Experimental section

2.1. Materials and methods

All chemicals were of best commercially available grade and used without further purification. Deuterohemin (Fe-DP) was produced according to the methods described in the literature [17]. Deuteroporphyrin (DP) was synthesized as previously described from hemin by demetalation of deuterohemin [18]. 2,7,12,18-tetramethyl-13,17-di(3-hydroxypropyl)porphyrin (DHPP) was

* Corresponding author. Tel./fax: +86 025 84315030.

E-mail addresses: hubingcheng@yahoo.com, hubingcheng210094@163.com (B. Hu).



Scheme 1. Synthesis of manganese 2,7,12,18-tetramethyl-13,17-di(3-hydroxypropyl nicotinate)porphyrin.

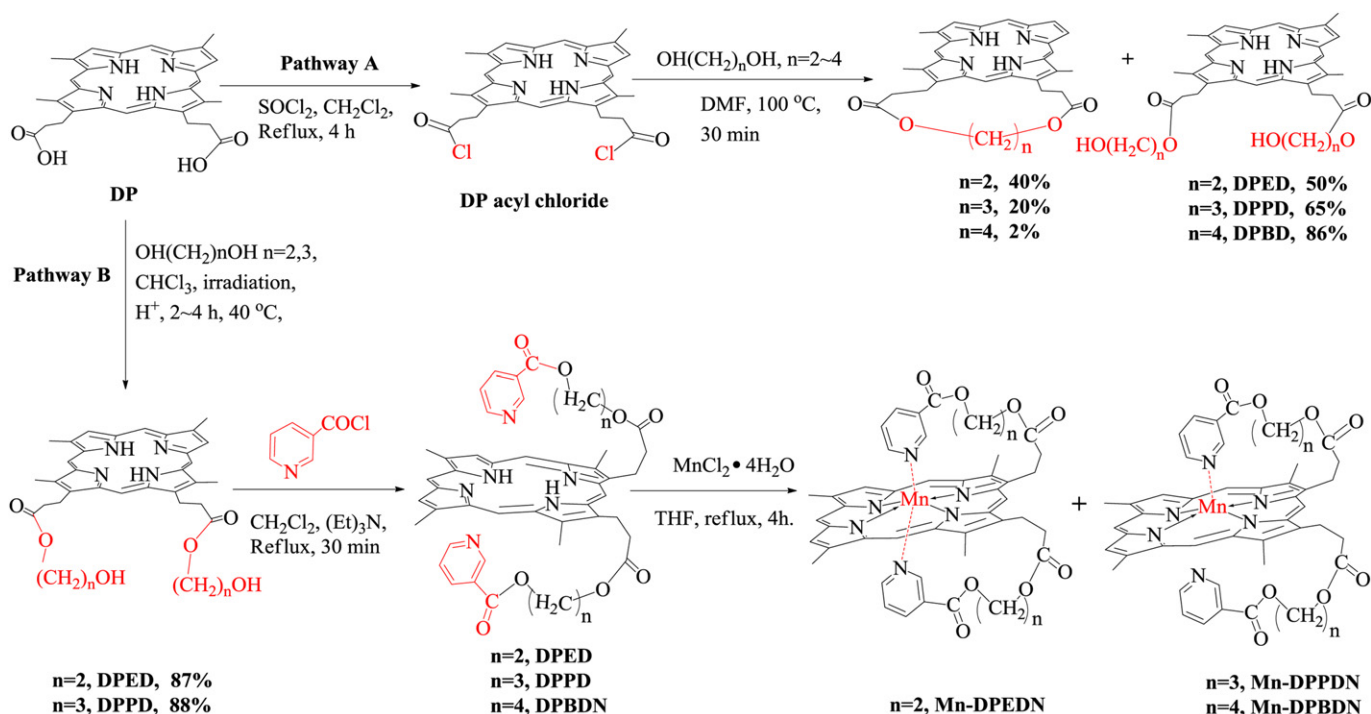
prepared as described in the literature [19]. ^1H NMR was recorded on a Bruker 500 MHz spectrometer. Elemental analysis was conducted on an PE-2004 (Perkin–Elmer) elemental analyzer. LC-MS/MS (ESI) mass spectra were recorded on a Finnigan TSQ Quantum ultra AM mass spectrometer. The UV–vis spectra were measured by a Shimadzu UV-240 spectrophotometer. IR spectra were obtained by a Bruker Tensor 27 spectrometer with KBr pellets. The electrochemical measurements were tested in a Chen Hua CHI 660 Electrochemical Workstation. Redox potentials of the compounds (10^{-3} mol/L) in dry *N,N*-dimethylformamide (DMF) containing 0.1 mol/L tetrabutylammonium perchlorate (TBAP) as supporting electrolyte were determined at room temperature by cyclic

voltammetry using platinum-carbon electrode, Pt and SCE as working, counter and reference electrodes, respectively.

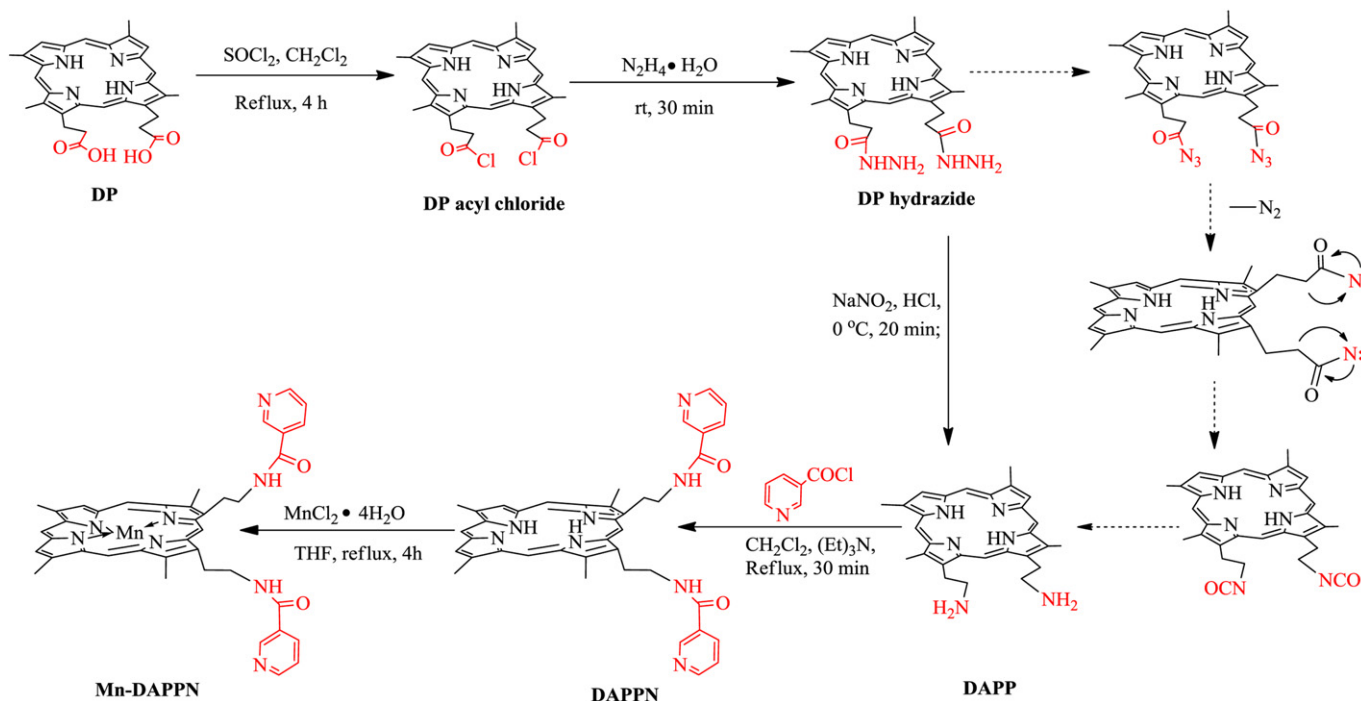
2.2. Synthesis

2.2.1. Synthesis of 2,7,12,18-tetramethyl-13,17-di(3-hydroxypropyl nicotinate)porphyrin (DPDN)

A dry CH_2Cl_2 (50 mL) solution of 2,7,12,18-tetramethyl-13,17-di(3-hydroxypropyl)porphyrin **DHPP** (0.30 g, 0.62 mmol) was added dropwise to nicotinoyl chloride (0.27 g, 1.91 mmol) and Et_3N (1 mL) in dry CH_2Cl_2 (10 mL). The mixture was stirred under reflux for 1 h. At the end of the reaction, the solution was cooled to room



Scheme 2. Synthesis of hydroxyl group-bridged manganese deuteroporphyrin-niacin dyads.



Scheme 3. Synthesis of manganese 2,7,12,18-tetramethyl-13,17-di(3-aminoethyl nicotinate)porphyrin.

temperature and washed with water. The precipitate was obtained by removing of solution and chromatographed on a silica gel column using dichloromethane/ethyl acetate = 5/2 (v/v) as the eluent. The main band was collected and dried at 50 °C for several hours in vacuo to give the compound **DPDN** as a black solid (0.38 g, 88%). $^1\text{H NMR}$ (500 MHz, CDCl_3): δ/ppm = -3.86 (s, 2H, NH); 2.74–2.79 (m, 4H, $\text{CH}_2\text{CH}_2\text{CH}_2\text{O}$); 4.21–4.25 (q, 4H, $\text{CH}_2\text{CH}_2\text{CH}_2\text{O}$); 4.64–4.67 (q, 4H, $\text{CH}_2\text{CH}_2\text{CH}_2\text{O}$); 3.62, 3.65, 3.75, 3.77 (4s, 12H, 4 CH_3); 6.87–6.90 (br, 2H, Py-5-H); 7.87–7.88 (d, 2H, Py-4-H); 8.51 (s, 2H, Py-6-H); 9.23 (s, 2H, Py-2-H); 9.09, 9.12 (2s, 2H, 3-, 8-H); 10.02–10.03 (d, 2H, 10-, 20-CH); 10.10, 10.13 (2s, 5H, 5-, 15-CH). ESI-MS/MS: $[\text{M} + \text{H}]^+ m/z$ (%) = 693.3913 (100). IR (KBr, ν/cm^{-1}): 3313(m), 2919 (m), 1719 (s), 1589 (s), 1419(w), 1384 (w), 1282 (s), 1233 (w), 1194 (w), 1130 (m), 1024 (s), 979 (w), 840 (w), 737 (s), 701 (w), 620 (w), 560 (w). Anal. Calcd for ($\text{C}_{42}\text{H}_{40}\text{N}_6\text{O}_4$): C, 72.81; H, 5.82; N, 12.13. Found: C, 72.70; H, 5.85; N, 12.21. UV-vis (CH_2Cl_2): 398, 497, 528, 565, 618.

2.2.2. Synthesis of deuteroporphyrin butanediol esters (**DPBD**)

To a stirred solution of 50 mL of dry CH_2Cl_2 containing 0.50 g of deuteroporphyrin **DP**, 0.5 mL of SOCl_2 was added. The resulting mixture was refluxed for 4 h. After evaporation, dry DMF (10 mL) and excess diols (10 mL) were added and heated at 100 °C for 30 min. At the end of the reaction, the mixture was poured into water. The residue was filtered, washed with water and purified by column chromatography on silica gel (dichloromethane:ethyl acetate = 5:3) to afford 0.55 g (0.84 mmol, 86%) of **DPBD** as a black solid. $^1\text{H NMR}$ (500 MHz, CDCl_3): δ/ppm = -3.88 (s, 2H, NH); 0.83–0.89 (m, 4H, $\text{COCH}_2\text{CH}_2\text{CH}_2\text{CH}_2\text{OH}$); 1.16–1.27 (m, 4H, $\text{COCH}_2\text{CH}_2\text{CH}_2\text{CH}_2\text{OH}$); 2.63–2.66 (t, 4H, J = 6.0 Hz, $\text{CH}_2\text{CH}_2\text{CO}$); 3.29–3.32 (t, 4H, J = 7.5 Hz, $\text{CH}_2\text{CH}_2\text{CO}$); 3.92–3.95 (t, 4H, J = 6.0 Hz, $\text{COCH}_2\text{CH}_2\text{CH}_2\text{CH}_2\text{OH}$); 4.44–4.48 (t, 4H, J = 7.5 Hz, $\text{COCH}_2\text{CH}_2\text{CH}_2\text{CH}_2\text{OH}$); 3.65, 3.68, 3.74, 3.77 (4s, 12H, 4 CH_3); 5.30 (s, 2H, OH); 9.11–9.13 (d, 2H, 3-, 8-H); 10.06, 10.10, 10.13, 10.18 (4s, 4H, 5-, 10-, 15, 20-CH). ESI-MS/MS: $[\text{M} + \text{H}]^+ m/z$ (%) = 655.1249 (100), $[\text{M} + \text{Na}]^+ m/z$ (%) = 677.1138 (15). IR

(KBr, ν/cm^{-1}): 3308 (s), 2920 (s), 2853 (w), 1731 (s), 1454 (m), 1361 (m), 1294 (w), 1233 (w), 1171 (s), 1107 (m), 1058 (m), 945 (m), 839 (m), 803 (w), 730 (m), 677 (m). Anal. Calcd for ($\text{C}_{38}\text{H}_{46}\text{N}_4\text{O}_6$): C, 69.70; H, 7.08; N, 8.56. Found: C, 68.81; H, 7.18; N, 8.85. UV-vis (CH_2Cl_2): 398, 495, 529, 563, 618.

2.2.3. Synthesis of deuteroporphyrin ethanediol/propanediol esters (**DPED** and **DPPD**)

To a solution of deuteroporphyrin (0.50 g, 0.98 mmol) and excess diol (10 mL) in CHCl_3 (10 mL) was added concentrated H_2SO_4 (0.7 mL) as catalyst at 40 °C in an ultrasound bath having a frequency of 40 kHz. After the addition, the mixture was irradiated by ultrasound for 4 h, the mixture was then extracted with CH_2Cl_2 (3 \times 100 mL). The organic layer was washed with water, dried over anhydrous Na_2SO_4 . After solvent removal, the residue was further purified by column chromatography on silica gel (dichloromethane:ethyl acetate = 5:3) to afford 0.51 g (0.85 mmol, 87%) and 0.54 g (0.86 mmol, 88%) of **DPED** and **DPPD** as black solids, respectively.

DPED: $^1\text{H NMR}$ (500 MHz, CDCl_3): δ/ppm = -3.87 (s, 2H, NH); 3.35–3.38 (t, 4H, J = 7.5 Hz, $\text{CH}_2\text{CH}_2\text{CO}$); 3.56–3.58 (q, 4H, $\text{CH}_2\text{CH}_2\text{CO}$); 4.16–4.18 (m, 4H, $\text{OCH}_2\text{CH}_2\text{OH}$); 4.45–4.48 (t, 4H, J = 7.5 Hz, $\text{OCH}_2\text{CH}_2\text{OH}$); 3.65–3.67, 3.75–3.78 (2d, 12H, 4 CH_3); 5.32 (s, 2H, OH) 9.11–9.12 (d, 2H, 3-, 8-H); 10.06, 10.10 (2s, 2H, 5-, 10-CH); 10.15–10.16 (d, 2H, 5-, 10-CH). ESI-MS/MS: $[\text{M} + \text{H}]^+ m/z$ (%) = 599.1732 (100), $[\text{M} + \text{Na}]^+ m/z$ (%) = 621.1992 (10), $[\text{M} + \text{K}]^+ m/z$ (%) = 637.0803 (3). IR (KBr, ν/cm^{-1}): 3414 (s), 3311(w), 2916 (w), 1731 (s), 1618 (m), 1382 (m), 1294 (w), 1232 (w), 1165 (s), 1077 (w), 892 (w), 840 (w), 731 (m), 676 (w), 620 (w). Anal. Calcd for ($\text{C}_{34}\text{H}_{38}\text{N}_4\text{O}_6$): C, 68.21; H, 6.40; N, 9.36. Found: C, 67.72; H, 6.58; N, 9.68. UV-vis (CH_2Cl_2): 398, 496, 529, 565, 618.

DPPD: $^1\text{H NMR}$ (500 MHz, CDCl_3): δ/ppm = -3.88 (s, 2H, NH); 1.39–1.46 (m, 4H, $\text{COCH}_2\text{CH}_2\text{CH}_2\text{OH}$); 2.81–2.87 (m, 4H, $\text{CH}_2\text{CH}_2\text{CO}$); 3.28–3.32 (t, 4H, J = 7.5 Hz, $\text{CH}_2\text{CH}_2\text{CO}$); 4.01–4.04 (q, 4H, $\text{COCH}_2\text{CH}_2\text{CH}_2\text{OH}$); 4.42–4.45 (t, 4H, J = 7.5 Hz, $\text{COCH}_2\text{CH}_2\text{CH}_2\text{OH}$); 3.63–3.66, 3.73–3.76 (2d, 12H, 4 CH_3); 5.29 (s,

2H, OH); 9.10–9.12 (d, 2H, 3-, 8-H); 10.04, 10.09, 10.15 (3s, 4H, 5-, 10-, 15, 20-CH). ESI-MS/MS: $[M + H]^+$ m/z (%) = 627.1695 (100), $[M + Na]^+$ m/z (%) = 649.1521 (5). IR (KBr, ν/cm^{-1}): 3418 (s), 3312 (m), 2919 (m), 1729 (s), 1619 (w), 1387 (m), 1271 (w), 1232 (w), 1167 (s), 1057 (m), 976 (m), 842 (m), 732 (m), 675 (w), 560 (w). Anal. Calcd for (C₃₆H₄₂N₄O₆): C, 68.99; H, 6.75; N, 8.94. Found: C, 68.91; H, 6.80; N, 8.90. UV–vis (CH₂Cl₂): 398, 496, 529, 565, 618.

2.2.4. Synthesis of deuteroporphyrin-niacin dyads (DPEDN, DPPDN and DPBDN)

The synthesis of **DPEDN**, **DPPDN** and **DPBDN** were similar to that of **DPDN** except that dichloromethane/ethyl acetate = 5/3 (v/v) for **DPBDN** was used instead of dichloromethane/ethyl acetate = 5/2 (v/v) as the eluent. **DPEDN**: 0.37 g (0.46 mmol, 91%); ¹H NMR (500 MHz, CDCl₃): δ/ppm = -3.99 (s, 2H, NH); 3.32–3.35 (t, 4H, J = 7.5 Hz, CH₂CH₂CO); 4.41–4.4 (t, 4H, J = 7.5 Hz, CH₂CH₂CO); 4.34–4.35 (br, 8H, CH₂CH₂OH); 3.61–3.63, 3.73–3.74 (2d, 12H, 4CH₃); 6.50–6.55 (m, 2H, Py-5-H); 7.48–7.81 (d, 2H, Py-4-H); 8.26–8.28 (t, 2H, Py-6-H); 8.84–8.85 (d, 2H, Py-2-H); 9.07–9.09 (d, 2H, 3-, 8-H); 9.98, 10.06 (2s, 2H, 5-, 10-CH); 10.09–10.10 (d, 2H, 5-, 10-CH). ESI-MS/MS: $[M + H]^+$ m/z (%) = 809.2950 (100), $[M + Na]^+$ m/z (%) = 831.2905 (20). IR (KBr, ν/cm^{-1}): 3310 (m), 2916 (m), 1725 (s), 1617 (w), 1590 (m), 1418 (m), 1378 (w), 1282 (s), 1237 (w), 1167 (m), 1135 (m), 1108 (m), 1025 (w), 946 (w), 897 (w), 840 (m), 738 (s), 704 (m), 677 (w), 621 (w). Anal. Calcd for (C₄₆H₄₄N₆O₈): C, 68.30; H, 5.48; N, 10.39; Found: C, 66.03; H, 5.51; N, 10.65. UV–vis (CH₂Cl₂): 398, 496, 529, 566, 618. **DPPDN**: 0.35 g (0.42 mmol, 87.5%); ¹H NMR (500 MHz, CDCl₃): δ/ppm = -3.91 (s, 2H, NH); 1.59 (br, 4H, OCH₂CH₂CH₂Opy); 3.28–3.31 (t, 4H, J = 7.5 Hz, CH₂CH₂CO); 4.01–4.04 (q, 4H, CH₂CH₂CO); 4.14–4.17 (t, 4H, J = 6.5 Hz, OCH₂CH₂CH₂Opy); 4.43 (t, 4H, J = 6.5 Hz, OCH₂CH₂CH₂Opy); 3.62–3.65, 3.71–3.74 (2d, 12H, 4CH₃); 7.10–7.13 (t, 2H, Py-5-H); 7.88–7.89 (d, 2H, Py-4-H); 8.63 (s, 2H, Py-6-H); 8.98 (s, 2H, Py-2-H); 9.06–9.07 (d, 2H, 3-, 8-H); 10.01–10.02, 10.10–10.11 (2d, 4H, 5-, 10-, 15, 20-CH). ESI-MS/MS: $[M + H]^+$ m/z (%) = 837.2686 (100). IR (KBr, ν/cm^{-1}): 3312 (m), 2921 (m), 1726 (s), 1592 (m), 1421 (w), 1383 (w), 1287 (s), 1234 (w), 1192 (w), 1164 (m), 1136 (m), 1050 (w), 1026 (w), 931 (w), 842 (w), 739 (m), 705 (w). Anal. Calcd for (C₄₈H₄₈N₆O₈): C, 68.88; H, 5.78; N, 10.04. Found: C, 69.01; H, 5.94; N, 9.76. UV–vis (CH₂Cl₂): 397, 496, 529, 565, 618. **DPBDN**: 0.35 g (0.41 mmol, 88%); ¹H NMR (500 MHz, CDCl₃): δ/ppm = -3.83 (s, 2H, NH); 1.28–1.35 (m, 4H, COCH₂CH₂CH₂CH₂OH); 1.43–1.48 (m, 4H, COCH₂CH₂CH₂CH₂OH); 3.29–3.32 (t, 4H, J = 7.5 Hz, CH₂CH₂CO); 3.77–3.81 (m, 4H, CH₂CH₂CO); 4.03–4.06 (m, 4H, COCH₂CH₂CH₂CH₂OH); 4.43–4.47 (q, 4H, COCH₂CH₂CH₂CH₂Opy); 3.64, 3.68, 3.72, 3.75 (4s, 12H, 4CH₃); 7.13–7.16 (q, 2H, Py-5-H); 7.87–7.90 (m, 2H, Py-4-H); 8.64–8.66 (m, 2H, Py-6-H); 8.96–8.98 (2d, 2H, Py-2-H); 9.07–9.09 (d, 2H, 3-, 8-H); 10.03–10.04, 10.14–10.15 (2d, 4H, 5-, 10-, 15, 20-CH). ESI-MS/MS: $[M + H]^+$ m/z (%) = 865.3849 (100), $[M + Na]^+$ m/z (%) = 887.5361 (5). IR (KBr, ν/cm^{-1}): 3312 (m), 2956 (m), 1724 (s), 1590 (m), 1419 (w), 1386 (w), 1285 (s), 1234 (w), 1164 (m), 1129 (m), 1025 (m), 972 (w), 840 (w), 739 (m), 704 (w), 676 (w), 619 (w). Anal. Calcd for (C₅₀H₅₂N₆O₈): C, 69.43; H, 6.06; N, 9.72. Found: C, 68.92; H, 6.19; N, 9.86. UV–vis (CH₂Cl₂): 397, 496, 529, 566, 618.

2.2.5. Synthesis of deuteroporphyrin hydrazide (DP hydrazide)

To a stirred solution of 50 mL of dry CH₂Cl₂ containing 0.30 g of deuteroporphyrin **DP**, 0.5 mL of SOCl₂ was added. The resulting mixture was refluxed for 4 h. After evaporation of the CH₂Cl₂ (more than 40 mL), excess hydrazine hydrate (10 mL, wt, 80%) was added dropwise and stirring was continued at ambient temperature for 30 min. Then, dilute sulfuric acid was added dropwise to the vigorously stirred suspension until the pH was brought to 8.0. The suspension was filtered and washed with water. The residue was

recrystallized from hot methanol and dried in vacuo at 100 °C for 3 h to afford **DP** hydrazide (0.30 g, 0.56 mmol, 95%). ¹H NMR (500 MHz, CDCl₃): δ/ppm = -4.05 (s, 2H, NH); 3.29–3.32 (t, 4H, J = 7.0 Hz, CH₂CH₂CO); 3.55–3.56 (d, 4H, NH₂) 3.62, 3.66, 3.73, 3.77 (4s, 12H, 4CH₃); 4.40–4.41 (m, 4H, CH₂CH₂CO); 5.76 (s, 2H, CONH); 9.33–9.35 (d, 2H, 3-, 8-H); 10.27–10.34 (3s, 4H, 5-, 10-, 15, 20-CH). ESI-MS/MS: $[M + H]^+$ m/z (%) = 539.0544 (100). Anal. Calcd for (C₃₀H₃₄N₈O₂): C, 66.89; H, 6.36; N, 20.80; Found: C, 65.71; H, 6.98; N, 20.61. UV–vis (DMF): 396, 495, 527, 565, 617.

2.2.6. Synthesis of 2,7,12,18-tetramethyl-13,17-di(3-aminoethyl)porphyrin (DAPP)

A solution of sodium nitrite (0.20 g, 2.90 mmol) in water (5 mL) was slowly added to a solution of the **DP** hydrazide (0.25 g, 0.46 mmol) in 0.5 M HCl (60 mL) at 0 °C. After dropping, the reaction was stirred for 20 min. The suspension was filtered, and the residue was washed with ice water and dried in vacuo at ambient temperature to give a puce solid. Toluene (20 mL) was added to the solid and refluxed for 5 min to generate N₂ gas and the concentrated HCl (1.5 mL) was added and refluxed for another 10 min to generate CO₂. Finally, the toluene was removed under reduced pressure to give the sticky liquid, which was neutralized with saturated aqueous NaHCO₃. The suspension was filtered and washed with water. The residue was purified by recrystallization from methanol to give **DAPP** (0.12 g, 0.27 mmol, 57%) as a black powder: ¹H NMR (500 MHz, CF₃COOD): δ/ppm = -4.25 (s, 2H, NH); 3.23 (t, 4H, J = 7.5 Hz, CH₂CH₂NH₂); 3.79–3.87 (4s, 12H, 4CH₃); 4.02 (s, 4H, CH₂CH₂NH₂); 4.66, 4.83 (2s, 4H, NH₂); 9.62–9.65 (t, 2H, 3-, 8-H), 10.97, 11.01, 11.09, 11.14 (4s, 4H, 5-, 10-, 15, 20-CH). ESI-MS/MS: $[M + H]^+$ m/z (%) = 453.0865 (100). Anal. Calcd for (C₂₈H₃₂N₆): C, 74.30; H, 7.13; N, 18.57; Found: C, 73.80; H, 7.82; N, 18.38. UV–vis (CH₃OH): 394, 495, 526, 565, 617.

2.2.7. Synthesis of 2,7,12,18-tetramethyl-13,17-di(3-aminoethyl)nicotinateporphyrin (DAPPN)

The synthesis of **DAPPN** was similar to that of **DPDN** except that dichloromethane/methanol = 10/1 (v/v) was used instead of dichloromethane/ethyl acetate = 5/2 (v/v) as the eluent. **DAPPN**: (0.31 g, 0.47 mmol, 71%), ¹H NMR (500 MHz, CDCl₃): δ/ppm = -3.85 (s, 2H, NH); 4.21 (br, 4H, CH₂CH₂NH); 4.32 (br, 4H, CH₂CH₂NH); 3.62–3.64, 3.71–3.74 (2d, 12H, 4CH₃); 5.30 (s, 2H, CH₂CH₂NH); 7.62–7.68 (br, 2H, Py-5-H); 7.99–8.00 (d, 2H, Py-4-H); 8.71 (s, 2H, Py-6-H); 9.04 (s, 2H, Py-2-H); 9.08–9.09 (d, 2H, 3-, 8-H); 10.02, 10.06, 10.13, 10.38 (4s, 4H, 5-, 10-, 15-, 20-CH); ESI-MS/MS: $[M + H]^+$ m/z (%) = 663.1509 (100). IR (KBr, ν/cm^{-1}): 3312 (w), 3059 (w), 2920 (m), 1655 (s), 1591 (s), 1543 (m), 1474 (w), 1417 (w), 1383 (w), 1269 (m), 1235 (m), 1195 (w), 1153 (w), 1023 (m), 977 (m), 850 (m), 735 (m), 705 (m), 625 (w). Anal. Calcd for (C₄₀H₃₈N₈O₂): C, 72.49; H, 5.78; N, 16.91. Found: C, 71.89; H, 5.97; N, 17.22. UV–vis (CH₂Cl₂): 400, 498, 530, 568, 618, 655.

2.2.8. Synthesis of manganese porphyrins

The process of metalation of porphyrin was based on the method of Adler et al. [20]. Metalloporphyrins were synthesized by the reaction of deuteroporphyrin-niacin dyads (0.20 g) with MnCl₂·5H₂O (0.50 g) in tetrahydrofuran (50 mL) to afford high yields of more than 97%. The reaction conditions were stirred for 4 h under reflux. The process of metalation was monitored by UV–vis until the free base porphyrin was almost disappeared. After the completion of the reaction, the mixture was extracted with CH₂Cl₂ (300 mL). The organic layer was dried with magnesium sulfate and the solvents were evaporated. The crude compound was purified by chromatography on silica gel using CH₂Cl₂ and methanol (10/1 to 10/3) as the mobile phase.

Mn-DPDN: ESI-MS/MS: $[M]^+$ m/z (%) = 745.0766 (100). IR (KBr, ν/cm^{-1}): 2924 (m), 1721 (s), 1641 (s), 1549 (s), 1464 (m), 1422 (m), 1384 (s), 1327 (w), 1284 (m), 1131 (m), 1027 (m), 896 (w), 843 (w), 744 (w), 701 (w), 667 (w), 560 (w); UV–vis (CH_2Cl_2): 353, 470, 558, 771.

Mn-DPPD: ESI-MS/MS: $[M]^+$ m/z (%) = 707.2950 (100); UV–vis (CH_2Cl_2): 354, 469, 558, 768.

Mn-DPED: ESI-MS/MS: $[M]^+$ m/z (%) = 651.0128 (100); UV–vis (CH_2Cl_2): 352, 470, 558, 774.

Mn-DPPD: ESI-MS/MS: $[M]^+$ m/z (%) = 679.2384 (100); UV–vis (CH_2Cl_2): 352, 470, 558, 774.

Mn-DPEDN: ESI-MS/MS: $[M]^+$ m/z (%) = 861.1505 (100); IR (KBr, ν/cm^{-1}): 3049 (w), 2954 (w), 1727 (s), 1592 (m), 1422 (m), 1382 (w), 1228 (s), 1165 (m), 1132 (m), 1027 (m), 978 (w), 853 (w), 743 (m), 701 (w), 561 (w). UV–vis (CH_2Cl_2): 370, 471, 546, 799.

Mn-DPPDN: ESI-MS/MS: $[M]^+$ m/z (%) = 889.1945 (100); IR (KBr, ν/cm^{-1}): 3042 (w), 2922 (m), 1726 (s), 1592 (m), 1422 (w), 1384 (m), 1258 (s), 1167 (m), 1129 (m), 1028 (m), 977 (w), 929 (w), 853 (w), 745 (m), 702 (w), 634 (w); UV–vis (CH_2Cl_2): 361, 469, 553, 771.

Mn-DPBDN: ESI-MS/MS: $[M]^+$ m/z (%) = 917.2453 (100). IR (KBr, ν/cm^{-1}): 3049 (w), 2955 (m), 1725 (s), 1590 (s), 1419 (m), 1386 (m), 1355 (w), 1326 (m), 1285 (s), 1166 (m), 1128 (m), 1026 (m), 977 (w), 929 (w), 852 (w), 744 (m), 702 (w), 622 (w). UV–vis (CH_2Cl_2): 359, 470, 556, 771.

Mn-DAPPN: ESI-MS/MS: $[M]^+$ m/z (%) = 715.0444 (100), $[M + CH_3OH]^+$ m/z (%) = 747.0759 (15). UV–vis (CH_2Cl_2): 352, 473, 560, 799.

3. Results and discussion

3.1. Design and synthesis

As illustrated in Scheme 1, general synthetic procedures were used to construct the target molecules. In our first approach, Fe-DP was made from hemin, the extract of naturally occurring heme, according to the methods described in literature [17]. The deuteroporphyrin (DP) was synthesized from an aqueous HCl solution in acetic anhydride by demetalation of Fe-DP using a modified literature procedure [21], and purified it by recrystallization from acetone [18]. This modification avoided using large excess of gaseous HCl (or HBr) and laborious workup procedures including complicated and low yield-producing steps. It has the potential to be applied to the large-scale synthesis of similar porphyrin derivatives. The esterification of DP with methanol in the presence of concentrated sulfuric acid as a catalyst yielded the desired deuteroporphyrin dimethyl ester (DPDME). The reduction of DPDME by sodium borohydride and lithium chloride in dry THF solution gave 2,7,12,18-tetramethyl-13,17-di(3-hydroxypropyl) porphyrin (DHPP) in excellent yield [19]. Then, the DHPP reacted with an excess (3 equiv.) of nicotinoyl chloride in dry CH_2Cl_2 in the presence of $(Et)_3N$ for 1 h under reflux, which afforded the porphyrin-niacin dyad DPDN in 88% yield. DPDN was separated by column chromatography (silica gel) using dichloromethane/ethyl acetate (5:2) as the eluent.

Based on the above method, three compounds were prepared where the niacin moiety is directly bonded to the propionate side chains of deuteroporphyrin (Scheme 2). This method aimed to incorporate different numbers of carbon into the “bridge” that was used to link the porphyrin and niacin, and control the spatial distance between the ring of porphyrin and niacin. To the resulted double hydroxy porphyrins (DPED, DPPD and DPBD), diols were introduced at the position of propionate side chains of deuteroporphyrin as the key reaction. We chose pathway A in our first attempt for this purpose (Scheme 2). DP reacted with thionyl

chloride in dry CH_2Cl_2 to produce the high activity of DP acyl chloride. After removing of solvent, dry DMF and excess diols were added and heated at 100 °C for 30 min. When 1,2-ethanediol and 1,3-propanediol were employed in the second step, the reaction yielded only 50–65% of the expected porphyrin alcohol products along with a ring structure in the propionate side chains of porphyrin. However, when 1,4-butanediol was subjected to the above conditions, the double hydroxy porphyrin DPBD was generated as the major product with a negligible by-product. Pathway B was chosen to improve the reaction when the reactivity and structure of diols were taken into consideration. Under ultrasonic irradiation, the reaction of DP with 1,2-ethanediol and 1,3-propanediol in $CHCl_3$ was sluggish and required the addition of concentrated sulfuric acid to proceed to completion. DPED and DPPD were obtained for up to 4 h at 40 °C almost without any by-product. Conversion to the deuteroporphyrin-niacin dyads (DPEDN, DPPDN and DPBDN) was carried out in one step as shown in Scheme 2.

With the desired compounds DPDN–DPBDN in hand, we then found all of them with two long chains and the “bridge” was gradually increased with an increase in carbon number of diols. We attempted to shorten the carbon chain and designed the route for synthesis of 2,7,12,18-tetramethyl-13,17-di(3-aminoethyl) porphyrin (DAPP) via a three-step reaction (Scheme 3). First, DP acyl chloride was stirred at rt for 30 min with an excess of hydrazine hydrate (at 80wt.% hydrazine) to yield 95% DP hydrazide (after recrystallization from hot methanol). Second, DP hydrazide was treated with $NaNO_2$ under the standard conditions of Curtius rearrangement in an acidic medium to convert the hydrazide group of porphyrin to the porphyrin azide, which was then subjected to reflux under reaction solvent, thereby releasing nitrogen gas, finally converting acylazide group to an isocyanate group. Third, the isocyanate group was readily converted to an amino group DAPP in the presence of concentrated hydrochloric acid after hydrolysis. The target compound Mn-DAPPN was accessible to obtain with a total yield of 37% by following the above methods.

3.2. Optical properties

The UV–Vis spectra of the newly synthesized compounds are shown in Fig. 1. The deuteroporphyrin-niacin dyads exhibited typical intense Soret at ~398 nm and four weaker Q bands at ~496, 529, 566 and 618 nm with the exception of DAPPN, which contains an additional absorption peak at ~655 nm. In general, the

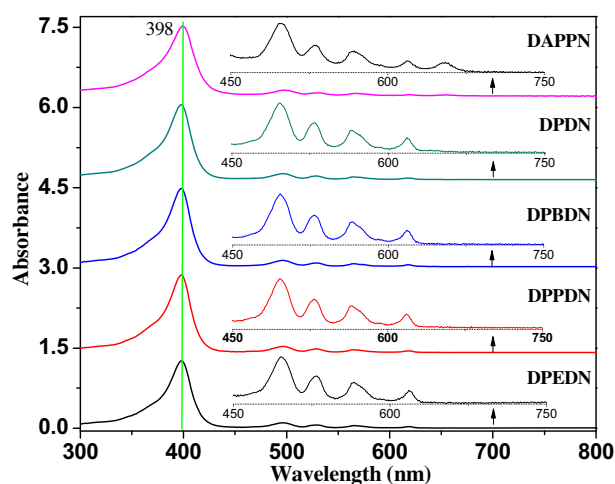


Fig. 1. Absorption spectra of deuteroporphyrin-niacin dyads.

Soret absorption peaks of these dyads were produced by electronic transitions from the ground state (S_0) to the lowest singlet excited state S_2 (Soret state). However, we did not observe any chain length effects on the Soret absorption peaks of these dyads, suggesting that there is no significant electronic communication between the niacin moiety and the ground state of the porphyrin ring. Notably, metalation of deuteroporphyrin-niacin dyads using $MnCl_2 \cdot 4H_2O$ in THF under reflux led to the successful insertion of metal ion onto the porphyrin core (confirmed by MS/MS and UV–Vis study), the effect of chain length could be observed prominently in the absorption spectra (Fig. 2). The Mn-DPEDN show a relatively more red shift of the Soret band compared to Mn-DPPDN and Mn-DPBDN along with the decrease of chain length, but the Q-bands show a relatively more blue shift. According to this phenomenon, the shorter the chain length that was used to link the porphyrin and niacin is, the more the red shift of the Soret band will become. However, opposite observations were made on the absorption spectra of the Mn-DPDN and Mn-DAPPN dyads. This phenomenon drew our attention to the coordination bonding interactions between the metal complexes and the N atoms of niacin.

In order to elaborate the intramolecular coordination of Mn(III) deuteroporphyrin-niacin dyads, Mn-DPED, Mn-DPPD and Mn-DPBD metal complexes as a model system without any niacin moiety were synthesized and investigated. This effect of niacin can be investigated by the addition of axial ligands with the similar structure to niacin. Methyl nicotinate and pyridine were selected as axial ligands for this purpose and compared the ligand-binding absorption spectra for manganese coordination before and after the metal complexation. As shown in Fig. 3, the spectral features of the Mn-DPED, Mn-DPPD and Mn-DPBD are very similar and exhibit a strong Soret band at ~ 352 nm. After adding methyl nicotinate (1 nmol, dissolved in 10 μ mL CH_3OH) into the reaction system, in situ determination reveals that the characteristic absorption peaks of these metal complexes are red shifted by ~ 5 nm (Soret band) compared to that of the parent Mn-DPED, Mn-DPPD and Mn-DPBD. These results were attributed to the axial coordination of methyl nicotinate to the manganese ion.

The absorption spectra of Mn-DPDN and Mn-DAPPN dyads, shown in Fig. 2, matched closely with those without methyl nicotinate observed in the reference system. Because the N atom of niacin is prohibited to coordinate manganese in Mn-DPDN and Mn-DAPPN dyads due to the short chain length. Furthermore, pyridine behaves as a strongly coordinating solvent, which is able to bind to

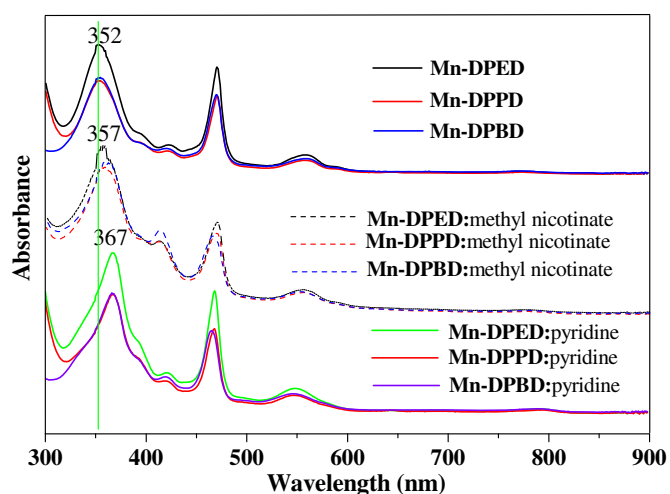


Fig. 3. Absorption spectra of Mn-DPED, Mn-DPPD and Mn-DPBD in the presence of methyl nicotinate and pyridine.

the metalloporphyrin and form six-coordinate complex. Lever et al. have reported that a solution of manganese porphyrin in coordinating solvent of pyridine is six-coordinate and low spin as shown by the ESR spectra [22].

Fig. 3 shows the typical spectral changes which take place in the Soret and Q band regions when pyridine (20 μ mL) is added to Mn-DPED, Mn-DPPD and Mn-DPBD. Their Soret bands are red shifted by about ~ 15 nm. Red shifts in the Soret band are commonly due to axial coordination of the N atom. However, the red shift of about ~ 15 nm in solution is much too large to be ascribed to the high spin and five-coordinate. Compared to the change of absorption spectra caused by adding the methyl nicotinate, the manganese is most possible six coordinate with two axial pyridines. Similar reactions that generate six coordinate manganese porphyrins can also be found in the literature [23]. Furthermore, Fig. 4 shows the gradual changes in the UV–vis spectra of Mn-DPED in the presence of varying amounts of pyridine, where the Soret peaks corresponding to Mn-DPED at 353 nm is decreasing in intensity, the Soret peak corresponding to the five-coordinate Mn-DPED(py) at 359 nm exhibits the lowest intensity and the Soret peak corresponding to

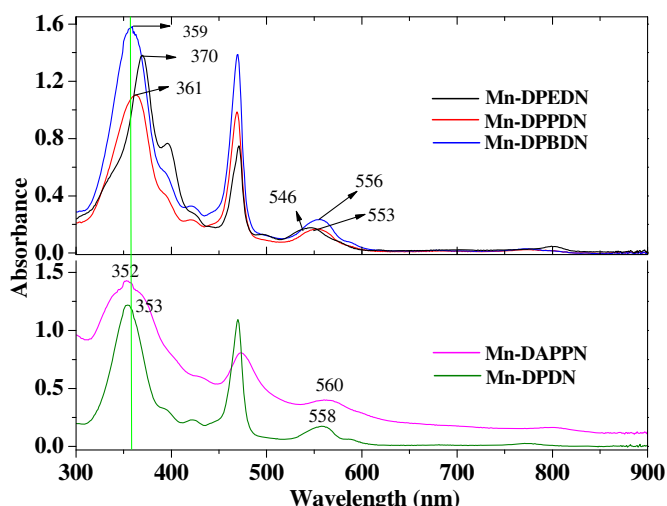


Fig. 2. Absorption spectra of manganese deuteroporphyrin-niacin dyads.

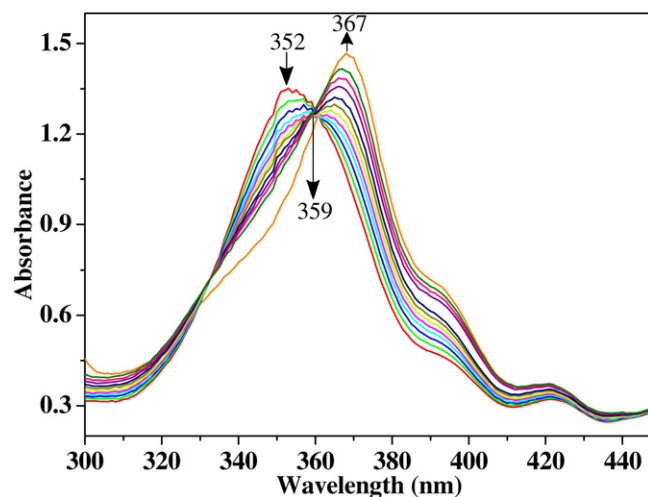


Fig. 4. Spectral change of Mn-DPED in dichloromethane in the presence of varying amounts of pyridine.

the six-coordinate Mn-DPED:(py)₂ at 367 nm is gaining in intensity.

It would be interesting to compare the above results with the absorption spectra of Mn-DPEDN, Mn-DPPDN and Mn-DPBDN. The absorption spectrum for Mn-DPBDN is essentially identical to that of the Mn-DPBD:methyl nicotinate complex, and the addition of pyridine resulted in the red-shift of the porphyrin Soret-band of Mn-DPED matched closely with Mn-DPEDN. These results suggest that the formation of intramolecularly complexed species depends on the length of the “bridge” in the double propionate side chains. There are two bent axial ligands in Mn-DPEDN due to the appropriate chain length. Oppositely, the long chains in Mn-DPBDN are difficult to simultaneously bind the manganese with two axial ligands, only bearing one axial ligand.

3.3. Electrochemical properties

According to the literature [24,25], Mn(III)porphyrins may be electrochemically reduced in a single electron transfer step to yield a porphyrin containing a Mn(II) central ion. The degree of axial ligation has a deep impact on the redox potential of Mn(III)/Mn(II). Fig. 5 shows the typical cyclic voltammograms at 100 mV/s in DMF/0.1 mol L⁻¹ tetrabutylammonium perchlorate (TBAP) obtained for Mn-DPEDN, Mn-DPPDN and Mn-DPBDN of this study. It also shows that the first oxidation process is chemically irreversible and the data analysis indicates a dramatic shift of redox peak along with different chain length. The $E_{1/2}$ values of Mn-DPEDN, Mn-DPPDN and Mn-DPBDN redox couples were -766.7, -760.5 and -750.4 mV, respectively. These data reflect the relative difference of Mn(III) toward axial coordination, caused by the strong interaction with the porphyrin ring. A comparison of the Mn-DPEDN and Mn-DPBDN dyads shows that the reduction of Mn(III) deuteroporphyrin-niacin dyads becomes more difficult by 16 mV as the degree of axial ligation is varied from five-coordination to six-coordination. The potential difference between cathodic and anodic peaks was 184.2 mV for the former and 172.8 mV for the latter. This indicates that the redox property of Mn-DPEDN was more irreversible than that of Mn-DPBDN. These results are in qualitative agreement with other studies which show complexation with one or two axial ligands led to an easier oxidation and a harder reduction compared to the uncomplexed four-coordinate manganese porphyrin species [26].

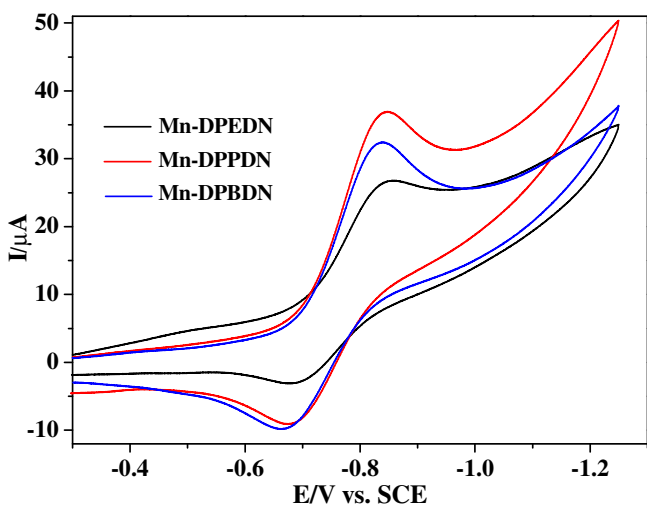


Fig. 5. Cyclic voltammograms of manganese deuteroporphyrin-niacin dyads in DMF + 0.1 mol/L TBAP.

4. Conclusions

We have described the synthesis of manganese deuteroporphyrin-niacin dyads with varying chain lengths via Curtius rearrangement and esterification of carboxyl group using diols as a “bridge” with different numbers of carbon. The behavior of intramolecular binding toward manganese porphyrin-niacin dyads generally depends on the chain lengths. Ultraviolet absorption spectra of Mn-DPBDN and Mn-DAPPN indicate that there is no interaction between the niacin and the Mn(III) center due to the short chains. In the presence of Mn-DPEDN, all of the pyridine units can bind to Mn(III) to form the six-coordinate complex. However, because of the long chains, as shown in Mn-DPBDN, only one pyridine unit is coordinately linked to the porphyrin ring.

Acknowledgments

The authors are grateful to Jiangsu Natural Science Foundation (No. BK2009386), NUST research funding (No. 2010GJPY043) and Jiangsu Graduate Innovation Project (CXZZ11_0263) for their financial support.

References

- Montellano PRO. Hydrocarbon hydroxylation by cytochrome P450 enzymes. *Chem Rev* 2010;110:932–48.
- Mora SJ, Cormick MP, Milanesio ME, Durantini EN. The photodynamic activity of a novel porphyrin derivative bearing a fluconazole structure in different media and against *Candida albicans*. *Dyes Pigm* 2010;87:234–40.
- Gonçalves EM, Bernardes CES, Diogo HP, Piedade MEM. Energetics and structure of nicotinic acid (niacin). *J Phys Chem B* 2010;114:5475–85.
- Jain P, Slama JT, Perez-Haddock LA, Walseth TF. Nicotinic acid adenine dinucleotide phosphate analogues containing substituted nicotinic acid: effect of modification on Ca_v2p release. *J Med Chem* 2010;53:7599–612.
- Intrieri D, Caselli A, Ragaini F, Macchi P, Casati N, Gallo E. Insights into the mechanism of the ruthenium-porphyrin-catalysed allylic amination of olefins by aryl azides. *Eur J Inorg Chem* 2012:569–80.
- Zou C, Zhang Z, Xu X, Gong Q, Li J, Wu CD. A multifunctional organic-inorganic hybrid structure based on Mn^{III}-porphyrin and polyoxometalate as a highly effective dye scavenger and heterogenous catalyst. *J Am Chem Soc* 2012;134:87–90.
- Qin J, Rao A, Chen X, Zhu X, Liu Z, Huang X, et al. Discovery of a potent nicotinic acid receptor agonist for the treatment of dyslipidemia. *ACS Med Chem Lett* 2011;2:171–6.
- Chapman MJ, Redfern JS, McGovern ME, Giral P. Niacin and fibrates in atherogenic dyslipidemia: pharmacotherapy to reduce cardiovascular risk. *Pharmacol Ther* 2010;126:314–45.
- Sun RJ, Cheng XL, Wang D, Zhuang CF, Xia AQ, Shi TS. Synthesis and properties of a series of porphyrin-niacin dyads and their Mn and Zn complexes. *J Coord Chem* 2009;62:1584–93.
- Santos FC, Cunha AC, Souza MCBV, Tomé AC, Neves MGPMS, Ferreira VF, et al. Synthesis of porphyrin-quinolone conjugates. *Tetrahedron Lett* 2008;49:7268–70.
- Cammidge AN, Lifsey KM. A simple synthesis of pyridine-tethered porphyrins. *Tetrahedron Lett* 2000;41:6655–6.
- Haycock RA, Hunter CA, James DA, Michelsen U, Sutton LR. Self-Assembly of oligomeric porphyrin rings. *Org Lett* 2000;2:2435–8.
- Visser J, Katsonis N, Vicario J, Feringa BL. Two-dimensional molecular patterning by surface-enhanced Zn-porphyrin coordination. *Langmuir* 2009;25:5980–5.
- Khvostichenko D, Yang QZ, Boulatov R. Simple heme dimers with strongly cooperative ligand binding. *Angew Chem Int Ed* 2007;46:8368–70.
- Traylor TG, Chang CK, Geibel J, Berzimis A, Mincey T, Cannon J. Syntheses and NMR characterization of chelated heme models of hemoproteins. *J Am Chem Soc* 1979;101:6716–31.
- D'Souza F, Hsieh YY, Deviprasad GR. Spectral and electrochemical investigations on the “Tail-On” and “Tail-Off” mechanism in pyridine covalently bound Zinc(II) porphyrins. *Inorg Chem* 1996;35:5747–9.
- Caughey WS, Alben JO, Fujimoto WY, York JL. Substituted deuteroporphyrins. I. reactions at the periphery of the porphyrin pin. *J Org Chem* 1966;31:2631–40.
- Sun CG, Hu BC, Zhou WY, Xu SC, Liu ZL. Investigations on the demetalation of metalloporphyrins under ultrasound irradiation. *Ultrason Sonochem* 2011;18:501–5.
- Sun CG, Hu BC, Zhou WY, Xu SC, Deng QZ, Liu ZL. Simple and efficient method for metallodeuteroporphyrin derivatives bearing symmetrical disulphide bond. *Chin Chem Lett* 2011;18:527–30.

- [20] Adler AD, Longo FR, Kampas F, Kim J. On the preparation of metallo-porphyrins. *J Inorg Nucl Chem* 1970;32:2443–5.
- [21] Espenson JH, Christensen RJ. Kinetics and mechanism of the demetalation of iron(III) porphyrins catalyzed by iron(II). *Inorg Chem* 1977;16:2561–4.
- [22] Lever ABP, Minor PC, Wilshire JP. Electrochemistry of manganese phthalocyanine in nonaqueous media. *Inorg Chem* 1981;20:2550–3.
- [23] Harvey JD, Ziegler CJ. Manganese N-confused porphyrin reactivity: CH bond activation and meso carbon reduction. *Chem Commun* 2003;2890–1.
- [24] Kadish KM, Kelly S. Electron-transfer and ligand-addition reactions of (meso-tetraphenylporphinato) manganese (II) and -manganese(III) chloride. *Inorg Chem* 1979;18:2968–71.
- [25] Kelly SL, Kadish KM. Counterion and solvent effects on the electrode reactions of manganese porphyrins. *Inorg Chem* 1982;21:3631–9.
- [26] Shen J, Ojaimi ME, Chkounda M, Gros CP, Barbe JM, Shao J, et al. Solvent, anion, and structural effects on the redox potentials and UV visible spectral properties of mononuclear manganese corroles. *Inorg Chem* 2008;47:7717–27.